Protein flexibility is key to cisplatin crosslinking in calmodulin

Huilin Li,[1] Stephen A. Wells,[2] J. Emilio Jimenez-Roldan,[2] Rudolf A. Römer,[2] Yao Zhao,[1] Peter J. Sadler,[1] and Peter B. O'Connor[1]*

[1]Department of Chemistry, University of Warwick, Coventry, CV4 7AL, United Kingdom
[2]Department of Physics and Centre for Scientific Computing, University of Warwick, Coventry, CV4 7AL, United Kingdom

Received 26 April 2012; Accepted 15 June 2012
DOI: 10.1002/pro.2111
Published online 25 June 2012 proteinscience.org

Abstract: Chemical crosslinking in combination with Fourier transform ion cyclotron resonance mass spectrometry (FTICR MS) has significant potential for studying protein structures and protein–protein interactions. Previously, cisplatin has been shown to be a crosslinker and crosslinks multiple methionine (Met) residues in apo-calmodulin (apo-CaM). However, the inter-residue distances obtained from nuclear magnetic resonance structures are inconsistent with the measured distance constraints by crosslinking. Met residues lie too far apart to be crosslinked by cisplatin. Here, by combining FTICR MS with a novel computational flexibility analysis, the flexible nature of the CaM structure is found to be key to cisplatin crosslinking in CaM. It is found that the side chains of Met residues can be brought together by flexible motions in both apo-CaM and calcium-bound CaM (Ca_4-CaM). The possibility of cisplatin crosslinking Ca_4-CaM is then confirmed by MS data. Therefore, flexibility analysis as a fast and low-cost computational method can be a useful tool for predicting crosslinking pairs in protein crosslinking analysis and facilitating MS data analysis. Finally, flexibility analysis also indicates that the crosslinking of platinum to pairs of Met residues will effectively close the nonpolar groove and thus will likely interfere with the binding of CaM to its protein targets, as was proved by comparing assays for cisplatin-modified/unmodified CaM binding to melittin. Collectively, these results suggest that cisplatin crosslinking of apo-CaM or Ca_4-CaM can inhibit the ability of CaM to recognize its target proteins, which may have important implications for understanding the mechanism of tumor resistance to platinum anticancer drugs.

Keywords: protein crosslinking; cisplatin; calmodulin; FTICR MS; flexibility simulation

Introduction

Proteins often carry out their function as part of large complexes, and their interactions are intrinsic to virtually every cellular process. Therefore, the determination of a protein's three-dimensional structure and the identification of its interaction partners are critical next steps in understanding protein action. Chemical crosslinking as a powerful tool for studying protein interactions has been used successfully for many years[1–5]; however, not until 2000, was the idea of combining crosslinking and mass spectrometry (MS) as a tool to study protein conformations and protein–protein interactions introduced by Young *et al.*[6] Since then, the developments in MS have greatly promoted the application of crosslinking in structural biology.[7–9] Fourier transform ion cyclotron resonance mass spectrometry (FTICR MS) has been shown to be a powerful tool for analyzing crosslinking in reaction mixtures, owing to its high

Additional Supporting Information may be found in the online version of this article.

Huilin Li and Stephen A. Wells contributed equally to this work.

Grant sponsors: NIH (NIH/NIGMS-R01GM078293); The ERC (247450); The Warwick Centre for Analytical Science (EPSRC funded EP/F034210/1); The Protein Biology and BioPhysics network; EPSRC (BP/G006792).

**Correspondence to:* Peter B. O'Connor, Department of Chemistry, University of Warwick, Coventry, CV4 7AL, United Kingdom. E-mail: p.oconnor@warwick.ac.uk

sensitivity, high mass accuracy, high resolving power, and the availability of multiple fragmentation techniques.[10–15] The combination of chemical crosslinking with FTICR MS not only yields information about protein–protein interactions but also reveals which residues within protein complexes are close to one another in space. The high mass accuracy of FTICR MS can dramatically reduce the number of candidates for crosslinking products, and in addition, its high resolution, the ability to provide a "gas phase" purification to accumulate low-intensity crosslinked product ions, and the ability to fragment large proteins or peptides extensively, are critical tools that allow the unambiguous assignment of the crosslinking products and localization of the crosslinking sites. However, the identification of the crosslinked products can still be laborious and time-consuming owing to the complexity of the reaction mixtures. To overcome these challenges, significant effort has been dedicated to the design of new functional crosslinkers that can enrich cross-linked products via affinity tags or facilitate the identification of crosslinked products by introducing MS-cleavable bonds.[16–18]

Previously, the ability of cisplatin to act as a potential protein crosslinker was explored and demonstrated using standard peptides and the 16.8 kDa protein calmodulin (CaM).[15] Some of the features of cisplatin as a potential crosslinking reagent are highlighted in the following sections.

Chemical specificity

Cisplatin is different from current crosslinking reagents in targeting new functional groups;[19] thioether and imidazole groups, which provide complementarities with existing crosslinkers. Lysine residues are the most commonly targeted crosslinking groups, and are often located on the surface of proteins. Hence, lysine crosslinking usually provides surface information on proteins. Unlike crosslinking reagents which only target hydrophilic groups, cisplatin also targets the hydrophobic residue methionine (Met). Met residues are often located in the interior of proteins; therefore, targeting Met residues potentially provides information on the core of protein complexes.

Compatibility with MS

Platinum(II) inherently has two positive charges which enhance the detection of crosslinked products. Higher charge states not only promote the detection of crosslinked products with less purification, but result in more comprehensive MS/MS fragmentation and can assist the assignment of modification sites. Moreover, the unique isotopic pattern of platinum (^{194}Pt [97.41%], ^{195}Pt [100%], ^{196}Pt [74.58%]) flags crosslinking products and modification sites by MS, allowing for easy visual identification of crosslinked products in a spectrum without significantly complicating the spectrum or the need for additional labeling procedures.

Homobifunctional or heterobifunctional reactive groups

Cisplatin is square-planar with four co-ordinated ligands. In principle, all four original ligands can be replaced. As well as binding to Met (S) and His (N) residues, cisplatin can also bind to the thiol group of Cys (S) and carboxylate (O) groups, which provides the flexibility for homobifunctional or heterobifunctional or even heterotetrafunctional crosslinking.

Spacer arm length

The Pt^{II} ligand bond angles are ca. 90°, with Pt—N bond lengths of ca. 2.0 Å, and Pt—S bond lengths ca. 2.3 Å; thus, the spacer arm length of cisplatin as a crosslinker ranges from ca. 2.8 ($2 \times \sqrt{2}$) to 4.6 Å (Supporting Information Figure S-1).[20] Distance constraints are critical for protein structure prediction. They provide an initial approximation of the distance between two linked groups. The longer the arm length, the more likely it is that more crosslinks will be observed; however, less accurate spatial information is obtained. In contrast, zero-length crosslinkers (crosslinking proteins without adding spacer arm atoms between two conjugated molecules) require almost direct contact of the crosslinkable sites. Thus, the spatial distance range of cisplatin makes it a useful complementary crosslinking reagent.[21]

Cleavability and solubility

Cleavability is important in studies involving biospecific interactions between two molecules, which allow the verification of the crosslinking reactions through identification of the crosslinked sites. Previously, collisionally activated dissociation (CAD) and electron capture dissociation of Pt crosslinked product have shown the cleavability of Pt—S or Pt—N bonds,[15,22] facilitating the localization of the crosslinked sites. In addition, cisplatin is a widely used clinical anticancer drug; it is water soluble (8 m*M*) and is able to penetrate membranes.

Structure and function of calmodulin

Calmodulin (CaM) is a conserved and ubiquitous calcium (Ca^{2+})-binding protein that senses changes in intramolecular calcium levels to co-ordinate the activity of at least 30 different target proteins in eukaryotic cells.[23] CaM contains nine Met residues out of 148 amino acids, four of them located at residues 36, 51, 71, and 72 in the N-terminal part of the protein and another four at residues 109, 124, 144, and 145 near the C-terminus. A ninth Met is located at position 76 in the linker region [Fig. 1(A)].[24–26] High-affinity Ca^{2+} binding to two EF-hand Ca^{2+}-binding motifs in

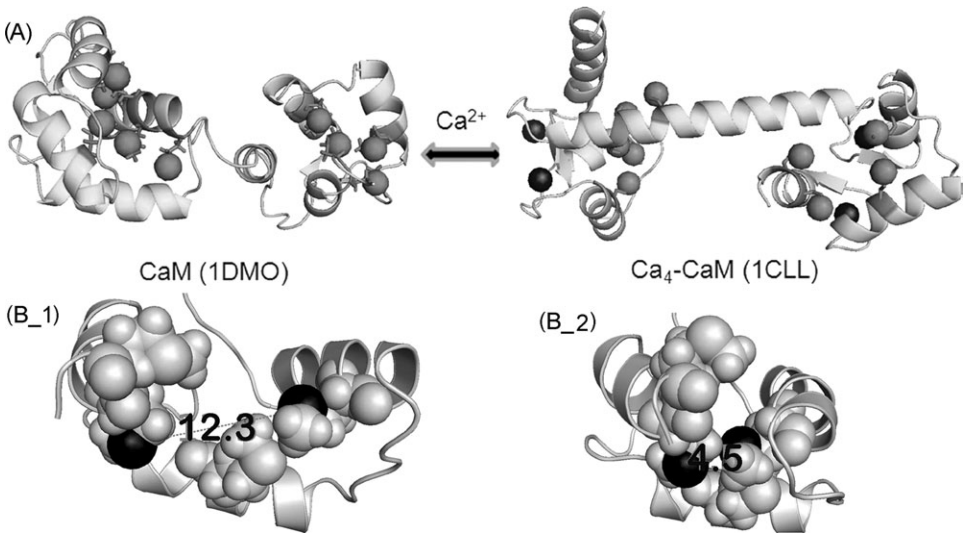

Figure 1. (A) NMR structure of CaM (1DMO, the first of 30 conformations)[25] and crystal structure of Ca_4-CaM (1CCL).[26] Calcium ions are in black, sulfur atoms Met residues indicated as spheres. (B) The C-terminal domain (residues, 80–147) of Ca_4-CaM (1CLL) shows the hydrophobic protein-binding groove: (B_1) at the start of a flexible-motion simulation (native structure), and (B_2) during flexible-motion simulation along mode m_{14}^- (Panel (B) is discussed in the *FRODA simulation results* section). The protein is mostly shown in cartoon view, with Met residues shown in all-atom view, and sulfurs highlighted in black. The sulfur–sulfur distance for residues 109 and 144 is shown as 12.3 Å at the start of a flexible-motion simulation (B_1) and 4.5 Å (B_2) during flexible-motion simulation along mode m_{14}^-. It is clear that these two residues have been brought into close proximity in mode 14^-.

each of the globular domains induces a conformational change from the more compact apo-CaM structure[25] to the more open Ca_4-CaM structure[26] as shown in Figure 1(A), which leads to the exposure of hydrophobic target-binding surfaces in each of the globular domains. Met residues contribute 46% of the exposed surface area of the hydrophobic patches on the calmodulin surface.[24] Previous results have shown that cisplatin crosslinks apo-calmodulin (apo-CaM) at multiple Met pairings, as follows: Met109–Met144, Met51–Met71/Met72, Met109–Met124, and Glu127/Asp129–Met144–Met145.[15,22] However, the distance constraints obtained from nuclear magnetic resonance (NMR) structures are inconsistent with the measured distance constraints from crosslinking (see Results and Supporting Information Table S-1). Our objective in this study is to resolve this inconsistency.

Protein structures generally are dynamic and flexible, displaying motion on a wide range of length and time scales.[27] In carrying out its biological function, CaM displays substantial flexibility in both the nonpolar binding grooves with the α-helical linker connecting the two globular domains; this flexibility is visible in NMR and simulations.[25,28–32] In particular, in a previous backbone dynamics study of calcium-saturated recombinant *Drosophila* CaM (the sequence of *Drosophila* CaM differences from the sequence of human CaM by 2 amino acids, F99-Y99, and S147-A147), Barbato *et al.* observed that a high degree of mobility exists near the middle of the central helix of CaM, and also in the loop that connects the first with the second EF-hand type calcium domain and in the loop connecting the third and fourth calcium-binding domains.[32] Back *et al.* pointed out that if a link originates from a residue localized in a flexible loop in the protein, attachments to residues scattered around the structure may be found.[9] However, it is not clear whether the crosslinks found to violate the distance constraints observed in the NMR structures of CaM can be attributed to observed mobility.[32]

Attempts to model large-scale dynamic motion at a very high level of theory (e.g., *ab initio* simulation) that could also describe the chemical details of the formation of Met—Pt bonds would be excessively computationally demanding. However, we expect the large-scale motion to be dominated by the intrinsic dynamics of the protein backbone,[27] and this motion can be investigated using simplified methods. In the present study, to assist in the interpretation of the experimental data, the flexible motion of CaM was modeled computationally, using a recently developed rapid method,[33] combining protein rigidity analysis,[34] geometric modeling of flexible motion,[35,36] and elastic network modeling[37] (details are explained in Supporting Information). These flexibility simulations allow us to explore large-amplitude motion along multiple normal modes in an all-atom protein structure at minimal computational expense[33] and provide valuable information on the geometry of potential platinum-binding sites. Results from flexibility simulations of Ca_4-CaM were further tested by additional MS experiments. Based on the results of crosslinking experiments and flexibility simulations,

Table I. *Predicted Crosslinking Sites as Obtained from Rigidity and Flexibility Analysis at Energy Cutoffs of −3 kcal/mol (for Results from Energy Cutoffs of −2 and −1 kcal/mol, see Supporting Information Table S-2a and b)*[a]

Rigidity cutoff −3 kcal/mol			+Ca structure (1CLL)			−Ca structure (calcium-deleted structure of 1CLL)		
Residue 1	Residue 2	$d(1-2)$ (Å) native(1CLL)	Mode of close approach	$d(1-2)$ (Å) simulated	MS experiment results	Mode of close approach	$d(1-2)$ (Å) simulated	MS experiment results
36	71	10.9	m_{13}^{+}	4.9	–			–
36	72	11.6			–	m_{13}^{+}	4.3	–
51	71	9.9	m_{13}^{+}	3.8	Yes	m_{13}^{+}	3.6	Yes
51	72	12.5			–			–
109	124	5.2	Many modes	<5	Yes	Many modes	<5	Yes
109	144	12.3	m_{14}^{-}	3.7	Yes	m_{14}^{-}	3.8	Yes
109	145	10.3			–			–
124	144	9.6	m_{18}^{+} m^{-}_{19}	4.1	–	m_{18}^{+}	4.6	–
124	145	11.0			–			–

[a] The first two columns give the potential crosslinking Met residues, the third shows the sulfur–surfur distance $d(1-2)$ obtained from the crystal structure of Ca_4-CaM (1CCL). The remaining columns show the modes in both +Ca and −Ca structures that can bring Met residues close to within 5 Å, and the corresponding $d(1-2)$ distances, and the MS results wherever available. "–" indicates that the crosslinking of the corresponding Met pairs was not observed in MS. (kcal/mol is used as a default unit in FIRST software, which can be converted to SI unit according to 1 kcal/mol = 4.2 kJ/mol).

a possible mechanism is suggested, by which the binding of anticancer drug cisplatin to CaM can decrease the ability of apo-CaM and Ca_4-CaM to recognize its target proteins.

Results and Discussion

Previously, Li *et al*. reported, using a combination of top-down and bottom-up MS methods, that cisplatin crosslinks multiple Met pairs of apo-CaM, as follows: Met51–Met71/Met72, Met109–Met124, Met109–Met144, and Glu127 or Asp129–Met144–Met145 (The detailed MS results are shown in Supporting Information Figure S-2 and the crosslinking pairs are listed in Table I).[15,22] However, the spatial distances of each crosslinked pair as determined from the reported family of 30 NMR structures of apo-CaM (Supporting Information Table S-1),[25] as sulfur–sulfur distances of each Met pair are as follows: Met51–Met71 (2.9–7.1 Å), Met51–Met72 (5.7–8.7 Å), Met109–Met124 (6.8–9.2 Å), Met109–Met144 (9.7–12.7 Å), and Met144–Met145 (5.2–9.2 Å). These values range from 2.9 to 12.7 Å; and only the spatial distances between Met51 and Met71 (in 11 conformations out of 30) fit the arm length range of cisplatin (2.82–4.63 Å).

Analysis of the crosslinking sites of cisplatin to CaM and Ca_4-CaM by flexibility approaches

Rigidity dilution analysis. Rigidity analysis is carried out in floppy inclusions and rigid substructure topography (FIRST) software, which predicts flexible regions in proteins by analyzing the constraints on flexibility formed by the covalent and noncovalent bonds.[38,39] Figure 2 shows the rigidity dilutions for the 1CLL CaM structure,[26] both in its native state including four bound calcium ions [Fig. 2(A)], and also in an edited state with calcium ions deleted from the structure [Fig. 2(B)]. In the native state, α-helical regions, for example, residues 103–111 (pink), 118–128 (green), 139–146 (blue), are generally visible as persistent rigid clusters during the dilution, and much of the N-terminal region remains a single rigid cluster to cutoff values around −2 kcal/mol (ca. 8.4 kJ/mol). However, the central helix (residues, 66–92) ceases to be a single rigid cluster at a cutoff of −1.178 kcal/mol. It appears that the capacity of the central helix to become flexible in CaM, visible in the NMR ensemble of structures 1DMO,[25] is predicted by the rigidity analysis.

Deletion of the calcium ions from the 1CLL structure [Fig. 2(B)] removes constraints from the network as protein–metal bonds are no longer present. The effects on the rigidity analysis are greatest at small values of the energy cutoff and are particularly visible in the N-terminal region. With calcium bound, residues 5–35 form as a solid robust helix structure [Fig. 2(A)]; upon removal of the calcium, the same region splits into two helices connected by a flexible linker region (residues, 19–30) [Fig. 2(B)]. The flexibility simulations were carried out using three different cutoffs (−1, −2, and −3 kcal/mol) for both the native- and the calcium-deleted structures. This allowed us to explore the flexible motion of the structure both when it is largely rigid and when it is largely flexible.[25]

Elastic network mode. Coarse-grained elastic network modeling[37] was performed to identify low-frequency modes of CaM based on its crystal structure (1CLL). The motions along the 20 lowest-

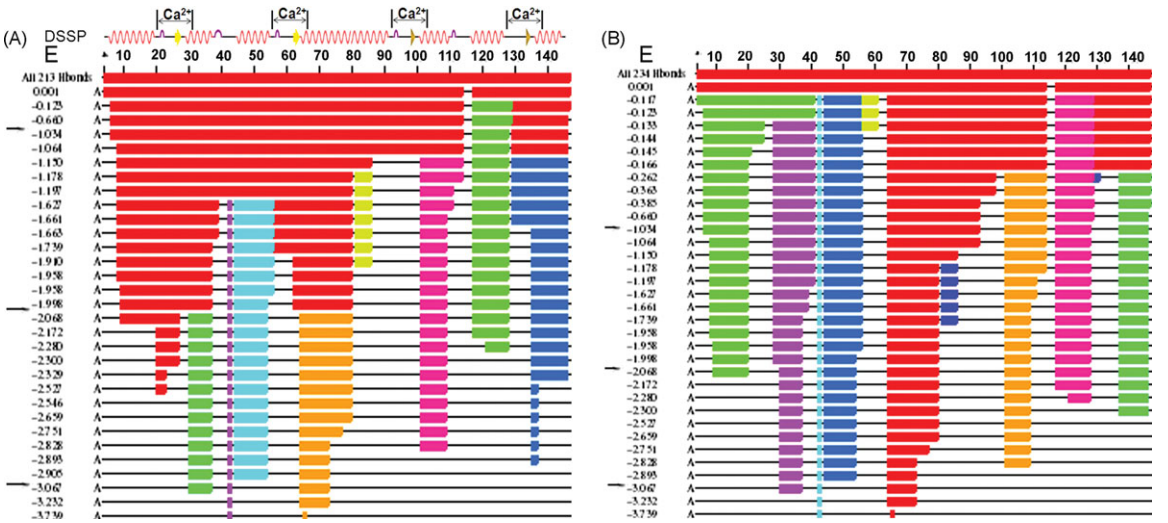

Figure 2. Rigidity dilution plots for (A) the native structure of Ca_4-CaM (1CLL), and (B) the Ca_4-CaM (1CLL) with calcium deleted. The primary sequence of the protein is represented as a line, and the secondary structure is presented by using DSSP (database of secondary structure assignments) with calcium-binding sites indicated.[40] A horizontal thin black line indicates a flexible region of the backbone, whereas a thick colored line indicates a rigid cluster. The topmost line of the plot shows the rigidity of the structure with the inclusion of all possible hydrogen bonds; the structure is almost entirely a single rigid cluster, shown in red. When E_{cut} is decreased (left-most column, in kcal/mol), rigid clusters break up as indicated in different colors and more of the chain becomes flexible (there are no correlations of the same colors between (A) and (B)). Cutoff values used in the simulation of flexible motion (−1, −2, and −3 kcal/mol) are indicated by arrows.

frequency nontrivial modes, that is, m_7–m_{26} were examined.† To distinguish between motion along the direction of a mode and motion opposite, m^+ and m^- were used, respectively. The protein displays a substantial amount of flexible motions along these modes. Some of these flexible motions bring pairs of Met residues into close proximity, potentially allowing crosslinking by cisplatin. As CaM is almost symmetric, several modes were found to occur in matched pairs, describing equivalent motions of the two globular domains.

FRODA simulation results. The FRODA software[34] was used to determine conformational changes in CaM. Each of the 20 mode eigenvectors of CaM was explored, in positive and negative directions, for each of three E_{cut} values, for the native- and calcium-deleted structures, making up 240 trajectories in all. The conformations generated in the flexibility simulations were examined and distances between the sulfur atoms of Met side-chains were extracted using a distance cutoff of 5 Å. Multiple cases were identified (Table I) in which a pair of sulfur atoms lying outside this cutoff distance in the crystal structure is brought within the cutoff by flexible motion along a mode eigenvector.

†Modes 1–6 represent combinations of rigid-body rotations and translations of the structure and have effectively zero frequency, so the lowest-frequency non-trivial mode is mode 7, hereinafter m_7.

In Figure 1(B), a flexible motion of the C-terminal globular domain is shown. The side chains of residues Met109 and Met144 are widely separated in the 1CLL crystal structure [Figure 1(B_1)], but are brought together by motion along m_{14} [Figure 1(B_2)], a mode that opens and closes the nonpolar binding groove. This suggests that the thioether side chains of Met109 and Met144 can co-ordinate to the same platinum ion when CaM binds to cisplatin. This would account for the observation of crosslinked fragments in MS, such as CaM(107–126) + Pt + CaM(127–148).[15]

Table I summarizes the results for significant pairs of Met residues in each domain, giving in each case the initial distance between the sulfur atoms, and the identity of any mode that brings the sulfur atoms within 5 Å of each other, along with the closest distance of approach in our simulations. In the N-terminal domain, the pairing of residues Met36–Met51 (Met(S)–Met(S) distance 4.97 Å) which are close in the 1CLL structure was neglected, and of residues Met71–Met72, that are adjacent in sequence. In the C-terminal domain, the pairing of residues Met144–Met145 was neglected as they are adjacent in sequence; for the pair of residues Met109–Met124, which are close in the native structure, multiple modes producing close approaches of this pair were found. Table I summarizes the data for simulations with and without calcium in the structure at the energy cutoff of −3 kcal/mol used in the rigidity analysis (results obtained at energy

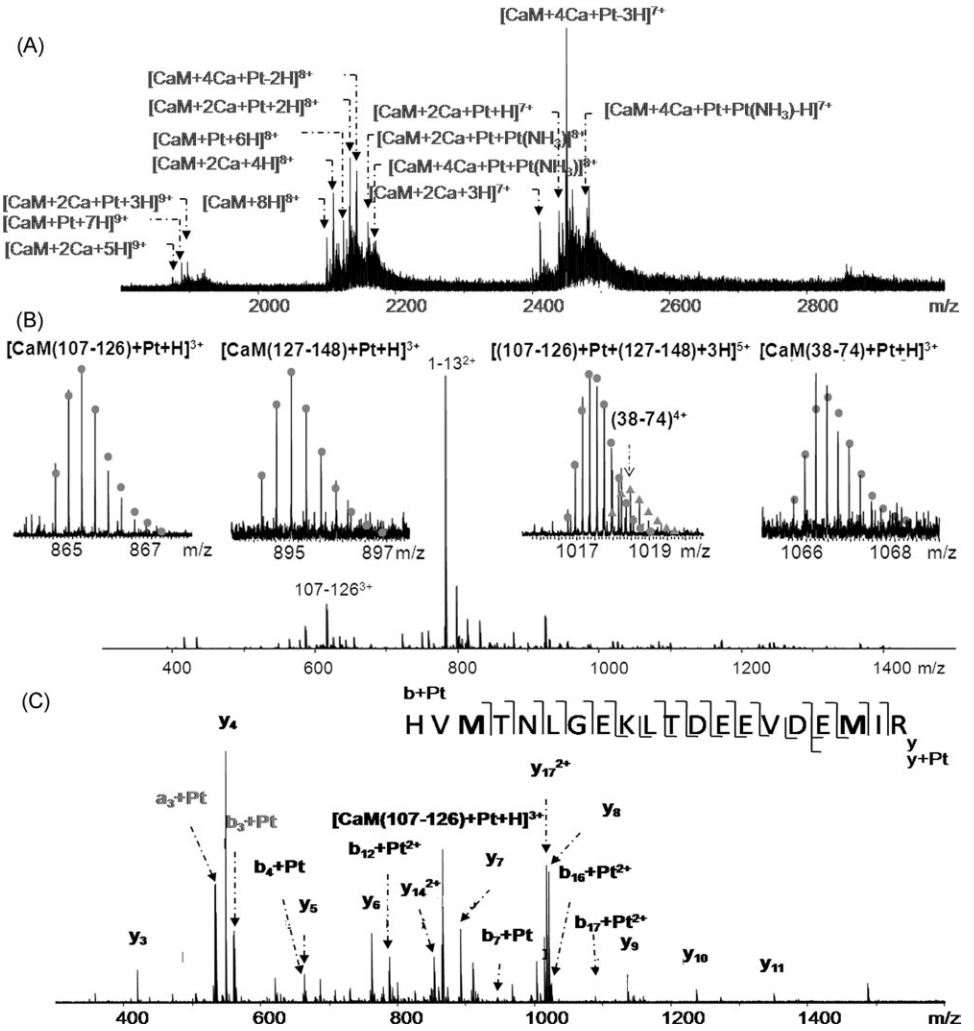

Figure 3. (A) Native ESI spectrum of Ca-CaM:cisplatin = 1:2 reaction products. (B) Trypsin digested Ca-CaM:cisplatin = 1:2 complex, the inserts are platinum crosslinked species; (C) CAD spectrum of $[CaM(107–126) + Pt + H]^{3+}$ species. The observation of $a_3 + Pt$ and $y_4 + Pt$ ions indicates that cisplatin crosslinks Met109 and Met124 residues.

cutoffs −2 and −1 kcal/mol are summarized in Supporting Information Table S-2). The holo-CaM (+Ca) structure is slightly less flexible than the apo-CaM (−Ca) structure; however, the residue pairings observed are consistent for both −Ca and +Ca CaM forms. The largest number of pairings was found at a cutoff of −3 kcal/mol and simulations at smaller cutoffs, when the protein is more rigid, have more restricted motion and produce fewer pairings (Supporting Information Table S-2a and b).

Mapping the binding sites of cisplatin to Ca_4-CaM by MS approaches

As summarized in Table I, the results obtained from flexibility analysis suggest that cisplatin can also crosslink Ca_4-CaM at multiple Met pairs. To test the predictions obtained from flexibility analysis experimentally, MS analysis of the products from reactions of cisplatin with calcium-containing CaM was carried out. Figure 3(A) shows the mass spectrum of reaction products of calcium-containing CaM with cisplatin (Ca-CaM:cisplatin = 1:2) under native spray conditions. Different calcium-binding forms of CaM were observed, mainly CaM + 2Ca and CaM + 4Ca. This is accounted for by the fact that the C-terminal lobe has a 10-fold higher Ca^{2+}-binding affinity than the N-terminal lobe.[41] More importantly, calcium-bound CaM displaced all four ligands from cisplatin, giving products such as CaM + Pt + 2Ca, CaM + 4Ca + Pt, and CaM + Pt + $Pt(NH_3)$ + 2Ca, which clearly indicates that cisplatin can also crosslink calcium-bound CaM. Subsequently, the Ca-CaM:cisplatin = 1:2 reaction products were further trypsin digested, and followed by MS analysis. Figure 3(B) shows that spectra from the trypsin-digested Ca-CaM:cisplatin = 1:2 sample contain a number of Pt-modified species. A common feature of the species shown in the insets of Figure

3(B), [CaM(107–126) + Pt + H]$^{3+}$ at m/z 865, [CaM(127–148) + Pt + H]$^{3+}$ at m/z 895, [CaM(107–126) + Pt + CaM(127–148) + 3H]$^{5+}$ at m/z 1018, and [CaM(38–74) + Pt + H]$^{3+}$ at m/z 1067, is that all the original ligands (NH_3 and Cl) of cisplatin have been displaced. This is attributable to the *trans*-labilization effect of Met sulfur.[42] The loss of two ammine ligands indicates that at least two Met residues bind to one platinum atom in each case. Therefore, cisplatin forms both interchain crosslinks CaM(107–126) and CaM(127–148) fragments, and intrachain crosslinks CaM(38–74), CaM(107–126), and CaM(127–148) fragments. To further localize the crosslinking sites, the crosslinked species were fragmented by CAD. As an example shown in Figure 3(C), the observation of a_3 + Pt and y_4 + Pt ions in the CAD spectrum of [CaM(107–126) + Pt + H]$^{3+}$ species suggests that cisplatin intrachain crosslinks CaM(107–126) at Met109 and Met124. Thus, cisplatin can crosslink calcium-bound CaM at the same sites as to CaM, namely, Met51–Met71/Met72, Met109–Met124, Met109–Met144, and Met144–Met145 (Table I), which is consistent with the prediction based on the flexibility simulation results as summarized in Table I.

As the flexibility analysis results indicate that cisplatin might also crosslink Met36–Met72, Met124–Met144, we then checked MS results to see whether corresponding peaks had been detected. No peaks corresponding to platinum crosslinking Met36 and Met72 were observed. Also, no fragment ions indicating that cisplatin crosslinks Met124 and Met144 were found in the tandem MS spectra of either CaM(107–126) + Pt + CaM(127–148) or CaM(107–126) + Pt + CaM(142–148) species. There are several reasons for a theoretically possible crosslink not being observed in MS, including its low intensity, unfavorable ionization, and unsuitable peptide length.

As Glu and Asp residues can also potentially coordinate platinum, we carried out an additional search for close approaches between the side-chain carboxylate groups of residues Glu127 and Asp129 with each other and with the Met sulfur atoms in the C-terminal domain. The side chain carboxylate group of Glu127 is brought within 5 Å of the side-chain sulfur atom of Met144 by multiple flexible modes, at all energy cutoffs studies, in both +Ca and −Ca structures. In the simulations, Glu127 was not observed to pair with Met145, and Asp129 not to pair with either Met144 or Met145. The experimental observation of Pt-crosslinked CaM(127–148) fragments can thus be explained by the formation of Glu127-Pt-Met144 crosslinks as observed in the simulations. However, the formation of Asp129–Pt–Met145 crosslinks in this fragment cannot be excluded. Therefore, overall, the crosslinking MS results of calcium-bound CaM are consistent with the flexibility analysis of Ca_4-CaM.

Biological insights from crosslinking experiments and flexibility analysis

Previously, Jarve and Aggarwal reported that the treatment of rats with the anticancer drug cisplatin can immunohistochemically reduce the level of the Ca_4-CaM complex.[43] In addition, an *in vitro* experiment using an analogue of CaM, Mero–CaM–1, showed that cis-diammine-diaquacisplatinum(II), a hydrolyzed form of cisplatin, inhibited the CaM conformational shift through a direct interaction with the CaM molecule. The authors concluded that distention of the stomach was due to the inhibition of neuronal nitric oxide synthase activation by a direct interaction between the cisplatin and the calcium-binding sites of the CaM molecule. However, our previous results show that Met(S) residues are the preferential cisplatin-binding sites rather than the calcium-binding sites (mainly Glu(E) and Asp(D) residues), although the binding of cisplatin to Glu and Asp residues can occur when the molar ratios of cisplatin to CaM are high.[22] Met residues in CaM play an important role in its versatility and functions. It has been widely reported that the oxidation of Met residues (especially Met144 and Met145) of CaM decreases the ability of CaM to activate target proteins owing to a large reduction in the conformational flexibility of the Met side chains. [44–47] Met residues account for nearly half the surface area of the hydrophobic patches of Ca_4-CaM, and function by providing a target-binding interface. As shown in Figure 1(A), the binding of calcium exposes the hydrophobic patches of Ca_4-CaM, which in general moves Met residues further away from each other compared to calcium-free CaM NMR structures. However, the results of the flexibility simulation suggest that the crosslinking of cisplatin to multiple Met sites on CaM will trap the binding groove in a closed state and prevent opening of the binding interface [Fig. 1(B)], decreasing the ability of Ca_4-CaM to recognize its target proteins.

Melittin-binding assay

To verify the hypothesis that the crosslinking in CaM or Ca_4-CaM induced by cisplatin may decrease the ability of CaM to recognize its target proteins, reaction products of CaM and cisplatin (CaM:cisplatin = 1:2), and calcium-containing CaM with cisplatin (Ca-CaM:cisplatin = 1:2) were further reacted with melittin at a molar ratio of 1:1. Melittin is one of the most potent inhibitors of CaM activity, and has been widely used to evaluate the ability of CaM to recognize its targets.[45–47] Figure 4 shows MS spectra of melittin reacting with Ca-CaM, (CaM:cisplatin = 1:2)–Ca (calcium added to assist the recognition of melittin), and Ca-CaM:cisplatin = 1:2 complexes. As shown in

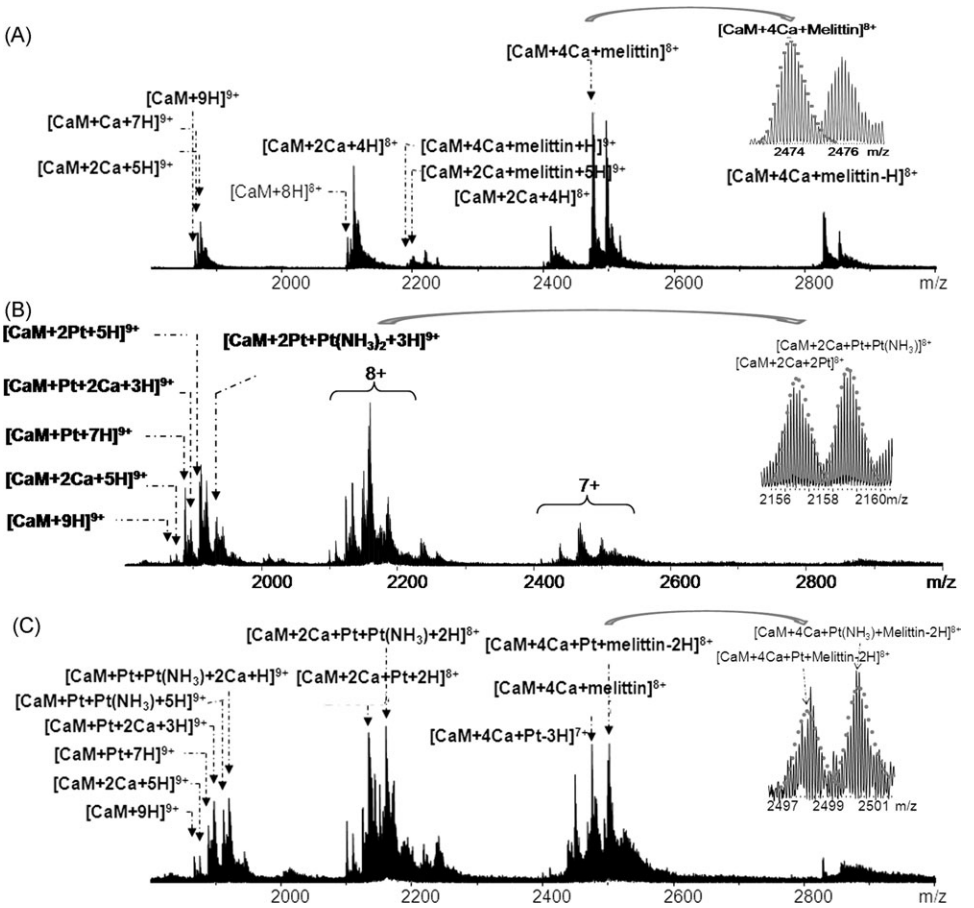

Figure 4. Native ESI spectra of protein complexes. (A) Ca-CaM:melittin = 1:1; (B) (CaM:cisplatin = 1:2)–Ca:melittin = 1:1; (C) (Ca–CaM:cisplatin = 1:2):melittin = 1:1.

Figure 4(A), the adduct Ca_4-CaM+melittin is the major product from the cisplatin-free CaM reaction; in addition, Ca_2-CaM also binds to melittin. On the contrary, as shown in Figure 4(B), once CaM has reacted with cisplatin, no peaks corresponding to Ca_4-CaM+melittin are detected when Ca^{2+} is added subsequently (with or without platinum, or different numbers of calcium ions).The spectrum is dominated by Pt-crosslinked CaM species; in addition, no crosslinked species were detected with four calcium ions bound. In comparison, for the case of calcium-bound CaM [Fig. 4(C)], the spectrum was dominated by platinum crosslinked CaM species; however, surprisingly, a species corresponding to CaM + 4Ca + Pt + melittin was observed (see the inset of Fig. 4(C)), which suggests that calcium binding opens up the more compact apo-CaM (calcium-free CaM) structure, as shown in Figure 1(A), increasing the exposure of hydrophobic target-binding surfaces in each of the globular domains. Therefore, even Pt-crosslinked Ca_4-CaM maintains an extended open structure, and thus maintains to a certain extent the ability to recognize its target, melittin. In contrast, the structures of calcium-free CaM are more compact, the crosslinking further closes the nonpolar groove. Therefore, addition of calcium ions after crosslinking cannot effectively change the structure of the Pt-crosslinked CaM species, and thus Pt-crosslinked CaM loses its ability to recognize its target.

Collectively, these results suggest that flexibility is key to cisplatin crosslinking in CaM. The crosslinking of cisplatin to apo-CaM or Ca-CaM can inhibit the ability of CaM to recognize its target proteins. In addition, the simulation of flexible motion can be a very useful tool for predicting crosslinking pairs in proteins and facilitating MS data analysis. In future studies, it will likely be instructive to refine these simulations here to further take account the fact that protein crosslinking by cisplatin occurs in a stepwise fashion on a time scale of minutes to hours. After the initial adduct $\{Pt(NH_3)_2Cl\}^+$ is formed with the protein, the charged cisplatin residue changes the local forces, adding new attractive charge–charge and charge–dipole interactions. Thus, these simulations likely underestimate both the reaction rate and the apparent distance over which cisplatin can crosslink proteins. Nevertheless, these cost-effective simulations can provide some structural and modal insight into the approach distances available in these proteins which helps to understand how crosslinking can occur over larger distances than initially expected. Ultimately, it is clear that such studies of platinated

proteins in a proteomic context will become increasingly important in the future as more platinum and metal-based therapeutics become available.

Experimental Procedures

Materials

Bovine calmodulin (CaM), trypsin (TPCK treated from bovine pancreas), melittin, calcium chloride ($CaCl_2$), ammonium acetate (CH_3COONH_4), and ammonium bicarbonate (NH_4HCO_3) were purchased from Sigma (St. Louis, MO). HPLC grade of methanol, acetic acid (HAc), and acetonitrile were obtained from Fisher Scientific (Pittsburgh, PA). Cisplatin was synthesized and characterized by a published method.[48]

Reaction of CaM and Ca-CaM with cisplatin

In the previous study, all the reactions were carried out in water.[15,22] Here, to simulate a physiological pH, all samples were reacted in 100 m*M* ammonium acetate (pH 6.8). Calcium-containing CaM was obtained by mixing a 500-μ*M* apo-CaM solution with a 50 m*M* $CaCl_2$ solution at a 1:10 volume ratio, yielding a calcium:CaM molar ratio of 1000:1. Ca-free CaM and Ca-containing CaM solutions were then subsequently reacted with cisplatin in a 1:2 molar ratio. The samples were incubated at 37°C for 24 h. To remove free platinum complexes and desalt, Amicon filters (MW cutoff = 3 kDa, Millipore, Watford, United Kingdom) were used at 13,000 rpm for 30 min at room temperature, and washed three times with 200 μL ammonium acetate (100 m*M*).

Reaction of Ca-CaM, apo-CaM–cisplatin complexes, and Ca-CaM–cisplatin complexes with mellitin

Ca-CaM, apo-CaM–cisplatin complexes with calcium added subsequently, and Ca-CaM–cisplatin adducts from the above experiments were mixed with melittin (1 m*M*) in 100 m*M* ammonium acetate at a molar ratio of 1:1, to give a final concentration of 20 μ*M* for each reaction complex. The same sample desalting procedure as described above was applied.

Digestion

The samples were diluted to 20 μ*M* with 50 m*M* NH_4HCO_3 (pH 7.8) and then subjected to trypsin digestion at a protein to enzyme ratio of 40:1 (w/w) at 37°C for 4 h. As a control, 20 μ*M* CaM without platinum reagents was digested under the same conditions.

FTICR MS

ESI-MS was performed on a Bruker solariX FTICR mass spectrometer with an ESI source and a 12 T actively shielded magnet. For native spray, the samples were diluted to 2 μ*M* with 100 m*M* ammonium acetate. For normal ESI analysis, the samples were diluted to 0.4 μ*M* with 50% MeOH-1% CH_3COOH buffer.

Flexible motion simulations

Rapid simulations of flexible motion were carried out by using a combination of protein rigidity analysis,[34] geometric modeling of flexible motion,[35] and elastic network modeling,[37] as described in detail in a recently developed method.[33] The input is an all-atom protein crystal structure. For Ca_4-CaM, the 1CLL crystal structure in the Protein Data Bank (PDB) was used,[26] with "REDUCE" (a program for adding hydrogens to a PDB molecular structure file)[49] to add hydrogens and PyMOL[50] to renumber all atoms.

Rigidity analysis

Rigidity analysis is carried out in floppy inclusions and rigid substructure topography (FIRST) using the pebble-game algorithm, which matches degrees of freedom against constraints to divide a molecular framework into rigid and flexible regions.[38,39] The constraints included are covalent bonds, hydrophobic tethers, and hydrogen bonds. Water molecules are not explicitly included but the assignment of noncovalent constraints assumes a polar solvent because of hydrophobic effects. The strength of hydrogen bonds was estimated in FIRST using a Mayo potential[51] based on donor–hydrogen–acceptor distance and angles. The set of hydrogen bonds to include in the analysis is selected using an energy cutoff value, E_{cut}. A rigidity dilution is carried out by gradually lowering E_{cut} from a value of 0 (including even the weakest hydrogen bonds) to a large negative value that excludes all but the strongest hydrogen bonds.[38,39] This provides information on the relative rigidity and flexibility of different portions of the structure, as in a recent study on the inhibition of HIV-1 protease,[52] and suggests values of E_{cut} in a physically relevant range to use in subsequent simulations of flexible motion.

Coarse-grained elastic network modeling in ElNemo[36]

This uses a one-site-per-residue representation of the protein structure, obtained from the PDB structure by selecting only the Cα atom of each residue. Springs of uniform strength are placed between all pairs of sites lying within a distance cutoff, in this case of 12 Å. Diagonalization of the resulting matrix generates a set of $3n$ elastic network modes (eigenvectors and frequency eigenvalues) for a protein structure of n residues; here $n = 144$ (the terminal residues 1–3 and residue 148 were not resolved in the 1CLL crystal structure).

The FRODA

The FRODA, implemented within FIRST, models bonding constraints in a molecular framework using a system of templates.[35,36] Motion is generated by a small

perturbation (typically of order 0.01 Å) of all atomic positions followed by reimposition of the bonding and steric constraints. To model flexible motion, an elastic network mode eigenvector was used as a systematic bias; the perturbation of the structure displaces all the atoms of a given residue in the direction of motion for that residue in the eigenvector. The process is iterated to produce a large amplitude of motion along the bias eigenvector while retaining physically reasonable bonding and steric geometry. Motions both parallel and antiparallel to the mode eigenvector were explored by using positive (+) and negative (−) biases. A trajectory of several thousand conformations, generating motion over several Ångström root-mean-square deviation, takes only a few central processing unit minutes, allowing for the rapid exploration of many modes.[33,40]

Acknowledgment

H. Li thankfully acknowledges a Warwick Postgraduate Research Scholarship (WPRS) and the Chemistry Department for Ph.D. studentship funding. S. A. Wells gratefully thanks the Leverhulme Trust for an Early Career Fellowship. The authors thank Dr. Mark P. Barrow for his help with the FTICR MS instrument and Dr. Weidong Cui for his instrument tuning suggestions using native spray. Financial support from NIH (NIH/NIGMS-R01GM078293), the ERC (247450), the Warwick Centre for Analytical Science (EPSRC funded EP/F034210/1), the Protein Biology and BioPhysics network, and EPSRC (BP/G006792) is gratefully acknowledged.

References

1. Manning LR, Morgan S, Beavis RC, Chait BT, Manning JM, Hess JR, Cross M, Currell DL, Marini MA, Winslow RM (1991) Preparation, properties, and plasma retention of human hemoglobin derivatives—comparison of uncrosslinked carboxymethylated hemoglobin with cross-linked tetrameric hemoglobin. Proc Natl Acad Sci USA 88:3329–3333.
2. Tobita H (1993) Kinetics of network formation in free-radical cross-linking copolymerization Macromolecules 26:5427–5435.
3. Hathout Y, Ellis T, Fabris D, Fenselau C (1996) Cross-linking of human placenta pi class glutathione S-transferase dimer by chlorambucil. Chem Res Toxicol 9: 1044–1049.
4. Zhu Q, Courtney, RJ (1988) Chemical crosslinking of glycoproteins on the envelope of herpes-simplex virus. Virology 167:377–384.
5. Steen H, Jensen ON (2002) Analysis of protein-nucleic acid interactions by photochemical cross-linking and mass spectrometry. Mass Spectrom Rev 21:163–182.
6. Young MM, Tang N, Hempel JC, Oshiro CM, Taylor EW, Kuntz ID, Gibson BW, Dollinger G (2000) High throughput protein fold identification by using experimental constraints derived from intramolecular cross-links and mass spectrometry. Proc Natl Acad Sci USA 97:5802–5806.
7. Rappsilber J, Siniossoglou S, Hurt EC, Mann M, (2000) A generic strategy to analyze the spatial organization of multi-protein complexes by cross-linking and mass spectrometry. Anal Chem 72:267275.
8. Bennett KL, Kussmann M, Bjork P, Godzwon M, Mikkelsen M, Sorensen P, Roepstorff P (2000) Chemical cross-linking with thiol-cleavable reagents combined with differential mass spectrometric peptide mapping—a novel approach to assess intermolecular protein contacts. Protein Sci 9:1503–1518.
9. Back JW, de Jong L, Muijsers AO, de Koster CG (2003) Chemical cross-linking and mass spectrometry for protein structural modeling. J Mol Biol 331:303–313.
10. Carlsohn E, Angstrom J, Emmett MR, Marshall AG, Nilsson CL (2004) Chemical cross-linking of the urease complex from Helicobacter pylori and analysis by Fourier transform ion cyclotron resonance mass spectrometry and molecular modeling. Int J Mass Spectrom 234: 137–144.
11. Sinz A, Kalkhof S, Ihling C (2005) Mapping protein interfaces by a trifunctional cross-linker combined with MALDI-TOF and ESI-FTICR mass spectrometry. J Am Soc Mass Spectrom 16:1921–1931.
12. Ihling C, Schmidt A, Kalkhof S, Schulz DM, Stingl C, Mechtler K, Haack M, Beck-Sickinger AG, Cooper DMF, Sinz A (2006) Isotope-labeled cross-linkers and Fourier transform ion cyclotron resonance mass spectrometry for structural analysis of a protein/peptide complex. J Am Soc Mass Spectrom 17:1100–1113.
13. Jacobsen RB, Sale KL, Ayson MJ, Novak P, Hong JH, Lane P, Wood NL, Kruppa GH, Young MM, Schoeniger JS (2006) Structure and dynamics of dark-state bovine rhodopsin revealed by chemical cross-linking and high-resolution mass spectrometry. Protein Sci 15: 1303–1317.
14. Wehr T (2006) Top-down versus bottom-up approaches in proteomics. LC GC North America 24:1004.
15. Li H, Zhao Y, Phillips HIA, Qi Y, Lin T-Y, Sadler PJ, O'Connor PB (2011) Mass spectrometry evidence for cisplatin ss a protein cross-linking reagent. Anal Chem 83:5369–5376.
16. Alloza I, Martens E, Hawthorne S, Vandenbroeck K (2004) Cross-linking approach to affinity capture of protein complexes from chaotrope-solubilized cell lysates. Anal Biochem 324:137–142.
17. Tang X, Bruce JE (2010) A new cross-linking strategy: protein interaction reporter (PIR) technology for protein-protein interaction studies. Mol BioSyst 6:939–947.
18. Tagwerker C, Flick K, Cui M, Guerrero C, Dou Y, Auer B, Baldi P, Huang L, Kaiser P (2006) A tandem affinity tag for two-step purification under fully denaturing conditions. Mol Cell Proteomics 5:737–748.
19. Sinz A (2006) Chemical cross-linking and mass spectrometry to map three-dimensional protein structures and protein-protein interactions. Mass Spectrom Rev 25:663–682.
20. Raudaschl G, Lippert B, Hoeschele JD, Howard-Lock HE, Lock CJL, Pilon P (1985) Adduct formation of cis-$(NH_3)_2PtX_2$ (X = Cl -, I -) with formamides and the crystal structure of cis-$(NH_3)_2PtCl_2(CH_3)_2NCHO$. Application for the purification of the antitumor agent cisplatin. Inorg Chim Acta 106:141–149.
21. Leitner A, Walzthoeni T, Kahraman A, Herzog F, Rinner O, Beck M, Aebersold R (2010) Probing native protein structures by chemical cross-linking, mass spectrometry, and bioinformatics. Mol Cell Proteomics 9:1634–1649.
22. Li H, Lin T-Y, Van Orden SL, Zhao Y, Barrow MP, Pizarro AM, Qi Y, Sadler PJ, O'Connor PB (2011) Use of top-down and bottom-up Fourier transform ion cyclotron resonance mass spectrometry for mapping

calmodulin sites modified by platinum anticancer drugs. Anal Chem 83:9507–9515.
23. Crivici A, Ikura M (1995) Molecular and structural basis of target recognition by calmodulin. Annu Rev Biophys Biomol Struct 24:85–116.
24. O'Neil KT, DeGrado WF (1990) How calmodulin binds its targets: sequence independent recognition of amphiphilic α-helices. Trends Biochem Sci 15:59–64.
25. Zhang M, Tanaka T, Ikura M (1995) Calcium-induced conformational transition revealed by the solution structure of apo calmodulin. Nat Struct Mol Biol 2: 758–767.
26. Chattopadhyaya R, Meador WE, Means AR, Quiocho FA (1992) Calmodulin structure refined at 1.7 Å resolution. J Mol Biol 228:1177–1192.
27. Henzler-Wildman K, Kern D (2007) Dynamic personalities of proteins. Nature 450:964–972.
28. Chou JJ, Li S, Klee, CB, Bax A. (2001) Solution structure of Ca^{2+}-calmodulin reveals flexible hand-like properties of its domains. Nature 8:990–997.
29. Yang C, Jas, GS, Kuczera, K (2004) Structure, dynamics and interaction with kinase targets: computer simulations of calmodulin. Biochim Biophys Acta 1697:289–300.
30. Thomas S, Tang X, Tapia L, Amato, NM (2007) Simulating protein motions with rigidity analysis. J Compt Biol 14:839–855.
31. Tripathi S, Portman JJ (2009) Inherent flexibility determines the transition mechanisms of the EF-hands of calmodulin. Proc Natl Acad Sci USA 106:2104–2109.
32. Barbato G, Ikura M, Kay LE, Pastor RW, Bax A (1992) Backbone dynamics of calmodulin studied by ^{15}N relaxation using inverse detected two-dimensional NMR spectroscopy: the central helix is flexible. Biochemistry 31:5269–5278.
33. Jimenez-Roldan JE, Freedman RB, Roemer RA, Wells SA (2012) Rapid simulation of protein motion: merging flexibility, rigidity and normal mode analysis. Phys Biol 9:016008.
34. Jacobs DJ, Rader AJ, Kuhn LA, Thorpe MF (2001) Protein flexibility predictions using graph theory. Proteins Struct Funct Bioinf 44:150–165.
35. Wells SA, Menor S, Hespenheide B, Thorpe MF (2005) Constrained geometric simulation of diffusive motion in proteins. Phys Biol 2:S127–S136.
36. Jolley CC, Wells SA, Hespenheide BM, Thorpe MF, Fromme P (2006) Docking of photosystem I subunit C using a constrained geometric simulation. J Am Chem Soc 128:8803–8812.
37. Suhre K, Yves-Henri S (2004) ElNémo: a normal mode web server for protein movement analysis and the generation of templates for molecular replacement. Nucleic Acids Res Suppl 1:W610–W614.
38. Hespenheide BM, Rader AJ, Thorpe MF, Kuhn LA (2002) Identifying protein folding cores from the evolution of flexible regions during unfolding. J Mol Graph Model 21:195–207.
39. Wells SA, Jimenez-Roldan JE, Roemer RA (2009) Comparative analysis of rigidity across protein families. Phys Biol 6:1–11.
40. Kabsch W, Sander C (1983) Dictionary of protein secondary structure: pattern recognition of hydrogen-bonded and geometrical features. Biopolymers 22: 2577–2637.
41. Wang CA (1985) A note on Ca^{2+} binding to calmodulin. Biochem Biophys Res Commun 130:426–430.
42. Kasherman Y, Sturup S, Gibson D (2009) Trans labilization of am(m)ine ligands from platinum(II) complexes by cancer cell extracts. J Biol Inorg Chem 14:387–399.
43. Jarve RK, Aggarwal SK (1997) Cisplatin-induced inhibition of the calcium-calmodulin complex, neuronal nitric oxide synthase activation and their role in stomach distention. Cancer Chemother Pharmacol 39:341–348.
44. Snijder J, Rose RJ, Raijmakers R, Heck AJR (2011) Site-specific methionine oxidation in calmodulin affects structural integrity and interaction with Ca^{2+}/calmodulin dependent protein kinase II. J Struct Biol 174:187–195.
45. Pan JX, Konermann L (2010) Calcium-induced structural transitions of the calmodulin-melittin system studied by electrospray mass spectrometry: conformational subpopulations and metal-unsaturated intermediates. Biochemistry 49:3477–3486.
46. Kataoka M, Head JF, Seaton BA, Engelman DM (1989) Melittin binding causes a large calcium-dependent conformational change in calmodulin. Proc Natl Acad Sci USA 86:6944–6948.
47. Comte M, Maulet Y, Cox JA (1983) Ca^{2+}-dependent high-affinity complex formation between calmodulin and melittin. Biochem J 1:269–272.
48. Dhara SC (1970) A rapid method for the synthesis of cis-$[Pt(NH_3)_2Cl_2]$. Indian J Chem 8:193–194.
49. Word JM, Lovell SC, Richardson JS, Richardson DC (1999) Asparagine and glutamine: using hydrogen atom contacts in the choice of side-chain amide orientation. J Mol Biol 285:1735–1747.
50. The PyMOL Molecular Graphics System, Publisher is Schrodinger LLC, URL is http://www.pymol.org.
51. Dahiyat BI, Benjamin GD, Mayo SL (1997) Automated design of the surface positions of protein helices. Protein Sci 6:1333–1337.
52. Heal JW, Jimenez-Roldan JE, Wells SA, Freedman RB, Römer RA (2012) Inhibition of HIV-1 protease: the rigidity perspective. Bioinformatics 28:350–357.
53. Jimenez-Roldan JE, Wells SA, Freedman RB, Roemer RA (2011) Integration of FIRST, FRODA and NMM in a coarse grained method to study protein disulphide Isomerase conformational change. Journal of Physics: Conference Series 286:1742–6588.